# Polarized Expression of Ion Channels and Solute Carrier Family Transporters on Heterogeneous Cultured Human Corneal Endothelial Cells

Junji Hamuro,[1] Hideto Deguchi,[1] Tomoko Fujita,[1] Koji Ueda,[2] Yuichi Tokuda,[3] Nao Hiramoto,[1] Kohsaku Numa,[1] Masakazu Nakano,[3] John Bush,[1] Morio Ueno,[1] Chie Sotozono,[1] and Shigeru Kinoshita[4]

[1]Department of Ophthalmology, Kyoto Prefectural University of Medicine, Kyoto, Japan
[2]Project for Personalized Cancer Medicine, Cancer Precision Medicine Center, Japanese Foundation for Cancer Research, Tokyo, Japan
[3]Department of Genomic Medical Sciences, Kyoto Prefectural University of Medicine, Kyoto, Japan
[4]Department of Frontier Medical Science and Technology for Ophthalmology, Kyoto Prefectural University of Medicine, Kyoto, Japan

Correspondence: Junji Hamuro, Department of Ophthalmology, Kyoto Prefectural University of Medicine, 465 Kajii-cho, Hirokoji-agaru, Kawaramachi-dori, Kamigyo-ku, Kyoto 602-0841, Japan; jshimo@koto.kpu-m.ac.jp.

**PURPOSE.** To clarify the expression profiles of ion channels and transporters of metabolic substrates among heterogeneous cultured human corneal endothelial cells (cHCECs) distinct in their effectiveness in reconstituting the corneal endothelium.

**METHODS.** Integrated proteomics for cell lysates by liquid chromatography–tandem mass spectrometry was carried out from three aliquots of cHCECs enriched in either cluster of definition (CD)$44^{-/+}$ (mature) cHCECs or $CD44^{++/+++}$ cell-state transition (CST) cHCECs. The expression profiles of cations/anions, monocarboxylic acid transporters (MCTs), and solute carrier (SLC) family proteins, as well as carbonic anhydrases (CAs), were investigated.

**RESULTS.** The polarized expression of cations/anions, MCTs, and SLC family proteins, as well as CAs, was clarified for mature and CST cHCECs. Most SLC4 family members, including SLC4A11 and SLC4A4 (NBCe1), were upregulated in the CST cHCECs, whereas SLC9A1 ($Na^+/H^+$ exchanger isoform one [NHE1]) and CA5B were detected only in the mature cHCECs. In addition, SLC25A42, catalyzing the entry of coenzyme A into the mitochondria, and SLC25A18, functioning as a mitochondrial glutamate carrier 2 (both relevant for providing the substrates for mitochondrial bioenergetics), were selectively expressed in the mature cHCECs.

**CONCLUSIONS.** Our findings may suggest the relevance of qualifying the polarized expression of these ion channels and transporter-like proteins to ensure not only the suitability but also the in vivo biological functionality of cHCECs selected for use in a cell-injection therapy.

Keywords: oxidative phosphorylation, glycolysis, mitochondria, ion channels, solute carrier family transporters

Corneal transplantations are among the most common and successful surgical procedures performed in modern-day medicine, with nearly 200,000 being performed globally each year. However, it is now anticipated that a novel and innovative cell-based regenerative medicine therapy involving the injection of cultured human corneal endothelial cells (cHCECs) will soon become an alternative surgical pathway to donor corneal graft transplantation for the treatment of corneal endothelial dysfunction.[1] Eight years ago, at the beginning of our study, there were very few published studies focused on investigating the phenotypical and functional heterogeneity of cHCECs. Thus, we first reported the presence of heterogeneity and a way to distinguish the heterogeneous cHCEC subpopulations by analyzing cluster of definition (CD) antigens expressed on their cell surface, and we defined the effector cells suitable for the therapy[2–4] (i.e., the SP with the $CD44^{-/+}CD166^+CD24^-CD26^-CD105^{low}$ phenotype).

The establishment of standardized quality control is a vital component for obtaining the required governmental approvals for legal-based pharmaceutical applications for safe, effective, and stable cell-based therapy. We conducted clinical studies that confirmed that the mature differentiated $CD44^{-/+}$ cHCECs exhibited a far better biological effect in the clinical setting than did cell-state transition (CST) cHCECs[1,2] (also see Ueno M, American Academy of Ophthalmology Annual Meeting, October 12, 2019, AAO E-Poster and Abstract PO070). However, it was important to deter-

mine, in detail, why and how the effector CD44$^{-/+}$ cHCECs exhibited a far better clinical outcome compared with CST cHCECs, which prompted us to conduct this current study to characterize the distinct cardinal features of CD44$^{-/+}$ and CST cHCECs with regard to the expression of ion channels and related transporters that may play pivotal roles in executing the in vivo biological effects.

Metabolically active corneal endothelial (CE) tissue helps to maintain corneal transparency via its ion and fluid transport properties. As we previously reported,[2] among the many ion channels the expression of Na$^+$/K$^+$ adenosine triphosphatase (ATPase) on cHCECs, alone, does not fully ensure in vivo biological functionality in a cell-injection therapy. From that aspect, the findings in a recent report by Li et al.[5] are quite instructive, as they illustrate that the transendothelial lactate gradient is required for efficient functioning of the Na$^+$/K$^+$-ATPase pump in CE tissues.

Mitochondrial respiration and glycolysis are the most relevant pathways for producing adenosine triphosphate (ATP), the primary molecular unit of intracellular bioenergetics in corneal endothelial cells (CECs), and are reportedly necessary for maintaining the corneal stroma in its adequately dehydrated and transparent state.[6–12] The ability of the cornea to maintain proper hydration is achieved by the balance between the passive leakage of fluid into the stroma and the active pumping of ions into the anterior chamber via metabolic energy.[6,13]

CE is one of the most metabolically active tissues in the human body.[14] In our recent study,[15] our findings revealed that the metabolic rewiring in mature differentiated cHCECs provides essential cues underlying the dynamics of cell fate modulation. In the previous preliminary studies, both Wang et al.[16] and our group[4] found that metabolomic profiling segregated immature from mature differentiated cHCECs. Moreover, our findings revealed that cHCECs have an inclination toward CST into a senescence phenotype, epithelial–mesenchymal transition, and transformed fibroblastic cell morphology, thus limiting their use in the clinical setting. CST cHCECs switch to a glycolytic metabotype, whereas mature differentiated cHCECs become more oxidative and elicit a reduced amount of lactate secretion extracellularly. The catabolic and anabolic pathways in the tricarboxylic acid (TCA) cycle operating in the mitochondrial matrix consist of multiple enzymes, such as citrate synthase, aconitase, isocitrate dehydrogenase, succinate dehydrogenase, fumarate hydratase, and malate dehydrogenase. We recently found that all of these isozymes function in the mitochondria of mature cHCECs, whereas the corresponding cytosolic isozymes function in CST cHCECs (Numa et al., manuscript in preparation).

In our previous study, we clarified the distinct expression profiles of CD44, c-Myc, and p53 among cHCECs.[2] Moreover, other recent studies have reported ammonia metabolism dictated by p53[17] and the identification of solute carrier (SLC) family protein 12A8 as a specific nicotinamide mononucleotide (NMN) transporter,[18] as well as an indication of the role of SLC4A11 in clinical etiology in late-onset Fuchs corneal dystrophy.[19] Thus, the purpose of this present study was to investigate the expression profiles in cHCECs of cations/anions, monocarboxylic acid transporters, and SLC family proteins, as well as carbonic anhydrases (CAs). Integral proteomics on cHCECs have revealed either up- or downregulated expression of these transporter-like proteins among cHCECs distinct in their phenotypes, and our findings may indicate the relevance of qualifying the polar-

ized expression of these ion channels and transporter-like proteins in order to clarify the in vivo pharmacological effect of cHCECs in a cell-injection therapy for CE disorders.

## MATERIALS AND METHODS

### Human Corneal Tissues and Endothelial Cell Donors

The human tissue used in this study was handled in accordance with the tenets set forth in the Declaration of Helsinki. HCECs were obtained from human donor corneas supplied by the CorneaGen (Seattle, WA, USA) eye bank and then cultured prior to the experimental analysis. Informed written consent for eye donation for research was obtained from the next of kin of all deceased donors. The donor eyes used for the culture were obtained from two donors: (1) age 27 years (corneal endothelial cell density [ECD], 3195 OD/3425 OS) and (2) age 11 (corneal ECD, 3202 OD/3588 OS). All four donor corneas used in this study were preserved in Optisol-GS (Chiron Vision, Inc., Irvine, CA, USA) and then shipped via international air transport for research purposes. Donor information accompanying the donor corneas showed that they were considered healthy and absent of any corneal disease.

### Cell Cultures of HCECs

HCECs obtained from the imported donor corneas were cultured according to the previously published protocols, yet with modifications.[2–4] Briefly, Descemet's membranes with CECs were stripped from the donor corneas and digested for 2 hours at 37°C with 1 mg/mL collagenase A (Roche Applied Science, Penzberg, Germany). The stripped HCECs were then seeded in one well of a six-well plate coated with Type I collagen (Corning, Inc., Corning, NY, USA). Culture medium was prepared according to previously published protocols.[2–4] The HCECs were then cultured at 37°C in a humidified atmosphere containing 5% CO$_2$, and the culture medium was changed twice per week. When the cHCECs had reached confluence, they underwent normal passaging at a density of 800 cells/mm$^2$ after treatment with TrypLE Select 10× (Thermo Fisher Scientific, Waltham, MA, USA) for 12 minutes at 37°C. The CD44$^{-/+}$ mature cHCECs and CD44$^{++/+++}$ CST cHCECs were derived from separate donors, as described above. The CD44$^{-/+}$ mature cHCECs were lysed after the 40-day culture, and the CD44$^{++/+++}$ CST cHCECs were lysed after the 135-day culture of the fourth passage. In our research, which extended for more than 4 years, we found that the only rational way to obtain CD44$^{-/+}$ mature cHCECs and CD44$^{++/+++}$ CST cHCECs from donors with the same range of donor age and tissue ECD was to prolong the culture period from the standard 35 to approximately 50 days to more than 130 days, with a change of medium every 3 to 4 days without culture passage (Supplementary Fig. S1). Three different lots of each culture for both subpopulations were lysed by the use of QIAzol Lysis Reagent (QIAGEN, Hilden, Germany).

### Flow Cytometry Analyses of the cHCECs

The cHCECs were collected from the culture dish via the above-described TrypLE Select treatment and then suspended at $4 \times 10^6$ cells/mL in flow cytometry (FACS) buffer (PBS containing 0.5% BSA and 0.05% NaN$_3$). Next,

an equal volume of antibody solution was added and then incubated for 2 hours at 4°C. The antibody solutions were as follows: fluorescein isothiocyanate (FITC)-conjugated anti-human CD26 mAb, PE-conjugated anti-human CD166 mAb, PerCP-Cy 5.5-conjugated anti-human CD24 mAb, PE-Cy 7-conjugated anti-human CD44, and FITC-conjugated antihuman CD90 mAb (all from BD Biosciences, San Jose, CA, USA), as well as APC-conjugated anti-human CD105 (eBioscience, Inc., San Diego, CA, USA). After washing with FACS buffer, the cHCECs were analyzed via use of the BD FACSCanto II Flow Cytometry System (BD Biosciences). The cell lysates of cHCECs at passage 4 were used for the proteome analysis. The mature cHCECs were collected from the three wells containing the population with a CD44$^{-/+}$ phenotype at the average ratio of 93.9%; similarly, the CST cHCECs were collected from the other three wells containing the population with a CD44$^{++/+++}$ phenotype at the average ratio of 73.8% (Supplementary Fig. S2).

## Reagents

Rho-associated protein kinase (ROCK) inhibitor Y-27632 and epidermal growth factor (EGF) were obtained from Wako Pure Chemical Industries, Ltd. (Osaka, Japan), and pyridinyl imidazole inhibitor SB203580 was obtained from Cayman Chemical (Ann Arbor, MI, USA). Dulbecco's Modified Eagle's Medium, High Glucose (DMEM-HG) and fetal bovine serum were obtained from Gibco Industries, Inc. (Langley, OK, USA), and plastic culture plates were obtained from Corning. Unless otherwise stated, all other chemicals were obtained from Sigma-Aldrich, Inc. (St. Louis, MO, USA).

## Integral Proteomics by Liquid Chromatography–Tandem Mass Spectrometry and Liquid Chromatography/Mass Spectrometry Dataset Analysis

All of the following procedures were performed as recently described.[15] In brief, the cell lysates of cHCECs at passage 4 were used for the proteome analysis. Three aliquots of each lysate from the three wells for either the mature cHCECs or CST cHCECs were analyzed. Cell lysates from three aliquots of each cHCEC were dried and resolved in 20 mmol/L HEPES-NaOH (pH 58.0), 12 mmol/L sodium deoxycholate, and 12 mmol/L sodium *N*-lauroylsarcosinate. After reduction with 20 mmol/L dithiothreitol at 100°C for 10 minutes and alkylation with 50 mmol/L iodoacetamide at ambient temperature for 45 minutes, proteins were digested with immobilized trypsin (Thermo Fisher Scientific). Peptides were analyzed using the LTQ Orbitrap Velos mass spectrometer combined with the UltiMate 3000 RSLCnano HPLC system (both, Thermo Fisher Scientific). Protein identification and quantification analysis were performed with MaxQuant software. The tandem mass spectrometry (MS/MS) spectra were searched against the *Homo sapiens* protein database in Swiss-Prot, with a false discovery rate set to 1% for both peptide and protein identification filters. Only Razor-unique peptides were used to calculate the relative protein concentrations. For the integral analysis of proteins, all detected peaks were standardized via the adjustment of the median value to 1.0 to 104.

The liquid chromatography (LC)/MS dataset, composed of 4641 proteins in total, was obtained using Proteome Discoverer 2.2 software.[15] After removal of the data for which the abundance ratio could not be calculated, we analyzed the remaining data by means of the web-based program DAVID v6.8 (The Database for Annotation, Visualization and Integrated Discovery; https://david.ncifcrf.gov). The data analysis resulted in 4315 genes, each with a unique DAVID Gene ID, for the subsequent analyses.

For gene expression analysis, we calculated the statistical *P* value and fold-change between two groups. Further investigations for the genes of interest, as well as the related genes and pathways suggested to be involved in cHCEC metabolism, were performed using DAVID and its BIOCARTA and KEGG_PATHWAY options.

## Statistical Analyses

In the LC/MS dataset analysis, the significance of difference between two types of cHCECs was assessed by Student's or Welch's *t*-test after confirmation by the *F* test. The fold-change was based on the abundance ratio derived from the Proteome Discoverer 2.2 software (Thermo Fischer Scientific). Microsoft Excel 2013 (Redmond, WA, USA) and R software version 3.6.0 (http://www.r-project.org/) were used for all data analysis.

## Measurement of Intracellular pH in cHCECs

In order to conduct a preliminary investigation of the presence or absence of a difference of intracellular pH (pHi) in cHCECs, either suitable or not for cell-injection therapy, pHi was measured from one specific CST cHCEC type via the use of the cell-permeable probe 3′-*O*-acetyl-2′,7′-*bis*(carboxyethyl)-5,6-carboxyfluorescein acetoxymethyl ester (BCECF-AM special packaging; Chemical Dojin, Co., Ltd., Tokyo, Japan). Two distinct cHCEC types were derived from the cornea of a 28-year-old female donor (ECD, 3003 cells/mm² and 3021 cells/mm², respectively), either in the presence of only 10-µM Y27632 and ascorbic acid in Nancy medium (mature cHCECs) or in the presence of 10-µM Y-27632 + 10-µM SB203580 + 5-ng/mL EGF + ascorbic acid (Sigma-Aldrich) in Nancy medium[3,4] for the first 4 days after cell seeding in each passage, as well as in the presence of these additives, except Y27632, for the later period of the culture (i.e., the CST cHCECs). The former consisted of 99.4% mature cHCECs, and the latter consisted of 100% CST cHCECs. The cHCECs were stained by use of the cell-permeable probe BCECF-AM, and all experiments were performed in accordance with the manufacturer's instructions. The fluorescence intensity was determined by using a fluorescent plate reader with an excitation wavelength of 488 nm (GloMax Explorer; Promega Corporation, Madison, WI, USA). The mature cHCEC measurements were repeated 24 times, and the CST cHCEC measurements were repeated 12 times. Statistically significant differences were then assessed via the Mann–Whitney *U* test.

In this study, we used Dojindo's assay kit (Dojindo Molecular Technologies, Inc., Tokyo, Japan). The procedures for calibrating BCECF fluorescence were as follows:

1. Prepare calibration buffer (130-mM KCl, 10-mM NaCl, 1-mM MgSO₄, and 10-mM Na-MOPS), pH 6.6, 7.0, 7.2, 7.4, 7.8, and 8.2.
2. Save 500 µL of cell suspension in a 1.5-mL PROTEOSAVE tube (Sumitomo Bakelite Co., Ltd., Tokyo, Japan).
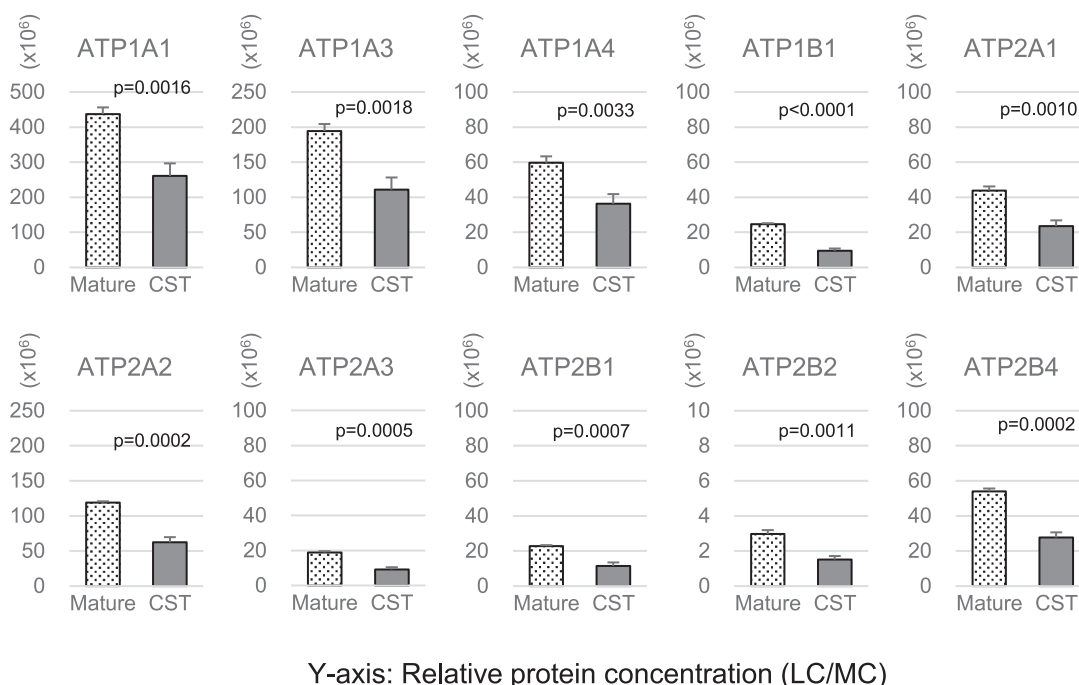
Y-axis: Relative protein concentration (LC/MC)

**Figure 1.** Protein expression levels of ATPase isoforms in mature and CST cHCECs. The average expression abundances of three lots of the mature cHCECs and CST cHCECs are shown. The significance of difference between the two types of cHCECs was assessed by Student's *t*-tests after confirmation by *F* tests. $P < 0.01$ was considered statistically significant. Integral proteomics on the two types of cHCECs revealed that the expression of all 11 isoforms was elevated more in the mature cHCECs than in the CST cHCECs. The CD44^{−/+} mature and CD44[++/+++] CST cHCECs were derived from two eyes of separate donors, as detailed in the text. Four culture passages were performed for both. To identify the cHCECs distinct to the expression of surface CD44, the CD44^{−/+} mature cHCECs were lysed at 40 days, and the CD44[++/+++] CST cHCECs were lysed at 135 days of the fourth passage.

3. Centrifuge two times at $300\times g$ (1867 rpm) for 3 minutes.
4. Suspend cell pellets in the six distinct pH calibration buffers.
5. Add 2.5 µL/500 µL of 2.2 mg/mL nigercin/EtOH (final concentration of 10 µg/mL), and incubate for 10 minutes at room temperature.
6. Pour 150 µL/well of prepared calibration cell suspension solution into a 96-well plate.
7. Measure with a fluorescence plate reader (GloMax Explorer; Promega, Madison, WI, USA), at 500-nm excitation and 530-nm detection.
8. Use 2 mg/mL nigercin/EtOH stock solution and 1-mM BCECF-AM/DMSO (Doujin Chemicals, Tokyo, Japan), 50 mg + 72.612 mL DMSO per B221 tube.

## RESULTS

### Na$^+$/K$^+$-ATPase Isomers

The expression of all 11 isoforms detected in the integral proteomics showed segregated profiles between cHCECs distinct in their cell surface phenotypes (i.e., CD44^{−/+} mature and CD44[++/+++] CST cHCECs), with CD44^{−/+} mature cHCECs exhibiting uniformly elevated expression of all 11 isoforms (Fig. 1), thus indicating that Na$^+$/K$^+$-ATPases are candidate components of the pump mechanism in the mature cHCECs, although the expression of this ATPase alone does not fully guarantee in vivo biological functionality when used for cell-injection therapy.[2] That finding immediately prompted us to explore the expression profiles of other ion channels, transporters, and SLC family proteins in cHCECs heterogeneous in their phenotypes.

### Nicotinate and Nicotinamide Metabolism

Oxidized nicotinamide adenine dinucleotide (NAD$^+$), which is required for the ATP-generating steps of glycolysis, is regenerated from NADH by mitochondrial NADH dehydrogenase or lactate dehydrogenase (LDH). NAD$^+$ biosynthesis is mediated mainly by nicotinamide phosphoribosyltransferase (NAMPT),[18,20] which catalyzes the conversion of nicotinamide and 5-phosphoribose pyrophosphate into nicotinamide mononucleotide (NMN).[21,22] We found that enzymes responsible for nicotinate and nicotinamide metabolism—NAMPT, purine nucleotide phosphorylase (PNP), nicotinamide *N*-methyltransferase (NNMT), and nicotinate phosphoribosyltransferase (NAPRT)—were all upregulated in the CST cHCECs, whereas only ectonucleotide pyrophosphatase/phosphodiesterase 1 (ENPP1) was upregulated in the mature cHCECs (Fig. 2).

### Arginine Metabolism and NH$_3$/H$^+$ Cotransporter SLC4A11

Recently, Zhang et al.[14] reported that glutaminolysis, the prerequisite for generating ATP to maintain CE function, is severely disrupted in CE cells deficient in SLC family 4 member 11 (SLC4A11), an NH$_3$/H$^+$ cotransporter, and that glutamine anaplerosis contributes to the additional supplies of biosynthetic precursors not met by glucose metabolism.
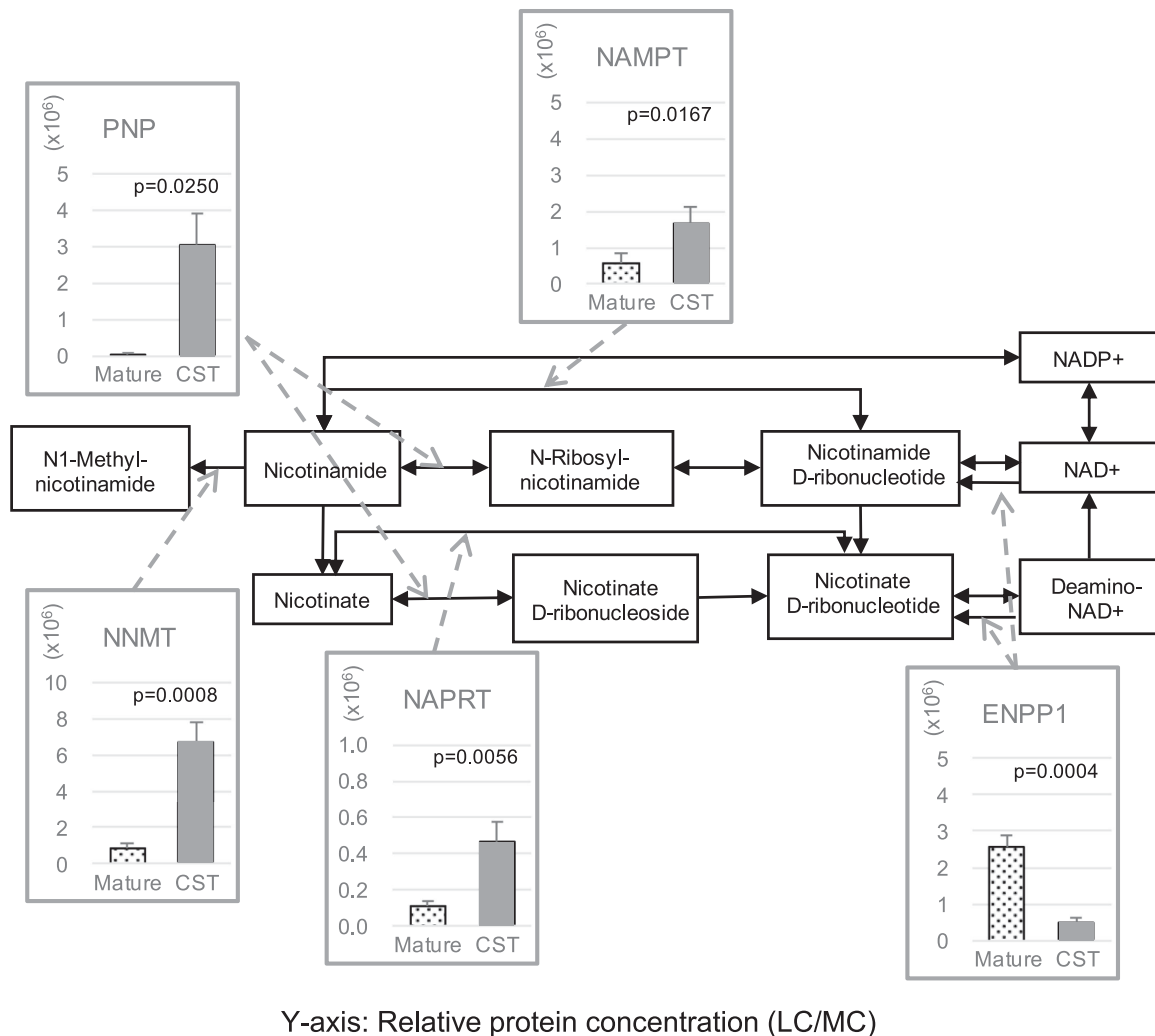
Y-axis: Relative protein concentration (LC/MC)

**Figure 2.** Protein expression levels of nicotinate and nicotinamide metabolites in mature and CST cHCECs. Segregated protein expression levels of key enzymes in nicotinate/nicotinamide metabolism in the two types of cHCECs are illustrated on the KEGG pathway map. The average expression abundances of three lots of mature cHCECs and CST cHCECs are shown. The significance of difference between the two types of cHCECs was assessed by Student's *t*-tests after confirmation by *F* tests. $P < 0.01$ was considered statistically significant. NAMPT, PNP, NNMT, NAPRT, and NY5C1A were upregulated in the CST cHCECs, whereas only ectonucleotide pyrophosphatase/phosphodiesterase 1 (ENPP1) was upregulated in the mature cHCECs. NT5C1A, 5′-nucleotidase, cytosolic IA; ND, not detected.

With that context in mind, in this current study we investigated nitrogen and arginine metabolism in cHCECs. Of note, we found that the expression of argininosuccinate synthase 1, known as the catalytic enzyme in the urea cycle (Fig. 3), as well as the expression of glutamate-ammonia ligase, was elevated in the CST cHCECs, in contrast with the reduced expression of glutamate dehydrogenase 1 and 2 and glutaminase 2 when compared with those in the mature cHCECs (Fig. 3).

Next, we investigated the expression of the SLC4 family members with regard to their roles in acid–base homeostasis. Our findings revealed that SLC4A4 was most abundantly expressed in cHCECs and that SLC4A11 was relatively more abundant than the other family members (Fig. 4). Interestingly, and in a sharp contrast with the enzymes involved in the arginine metabolic pathways, most of the five SLC4 family members detected were upregulated in the CST cHCECs (Fig. 4), including SLC4A11 and SLC4A4 (NBCe1), a sodium bicarbonate transporter, thus indicating

the presence of exquisite mechanisms for maintaining acid–base homeostasis in cHCECs heterogeneous in their phenotypes. SLC4A11 reportedly facilitates transmembrane water movement, $Na^+/OH^-$ co-transport, $Na^+$-independent $H^+$ ($OH^-$) transport, and $NH_3$ transport.[23] Intriguingly, although SLC9A1 ($Na^+/H^+$ exchanger isoform one [NHE1]), which is well known to be an $Na^+/H^+$ exchanger and crucial for pHi regulation,[24] was detected in the mature cHCECs but not in the CST cHCECs (Fig. 4).

## Nitrogen Metabolism and Carbonic Anhydrase

Considering the skewing of the CST cHCECs to a glycolytic metabotype in contrast to the skewing to mitochondrial oxidative phosphorylation of the mature cHCECs,[16] we were prompted to investigate the possible segregated expression of mitochondria carrier protein among cHCECs with distinct phenotypes. Similar to the findings in the previous reports,[13,25] we found that the absolute expression levels of
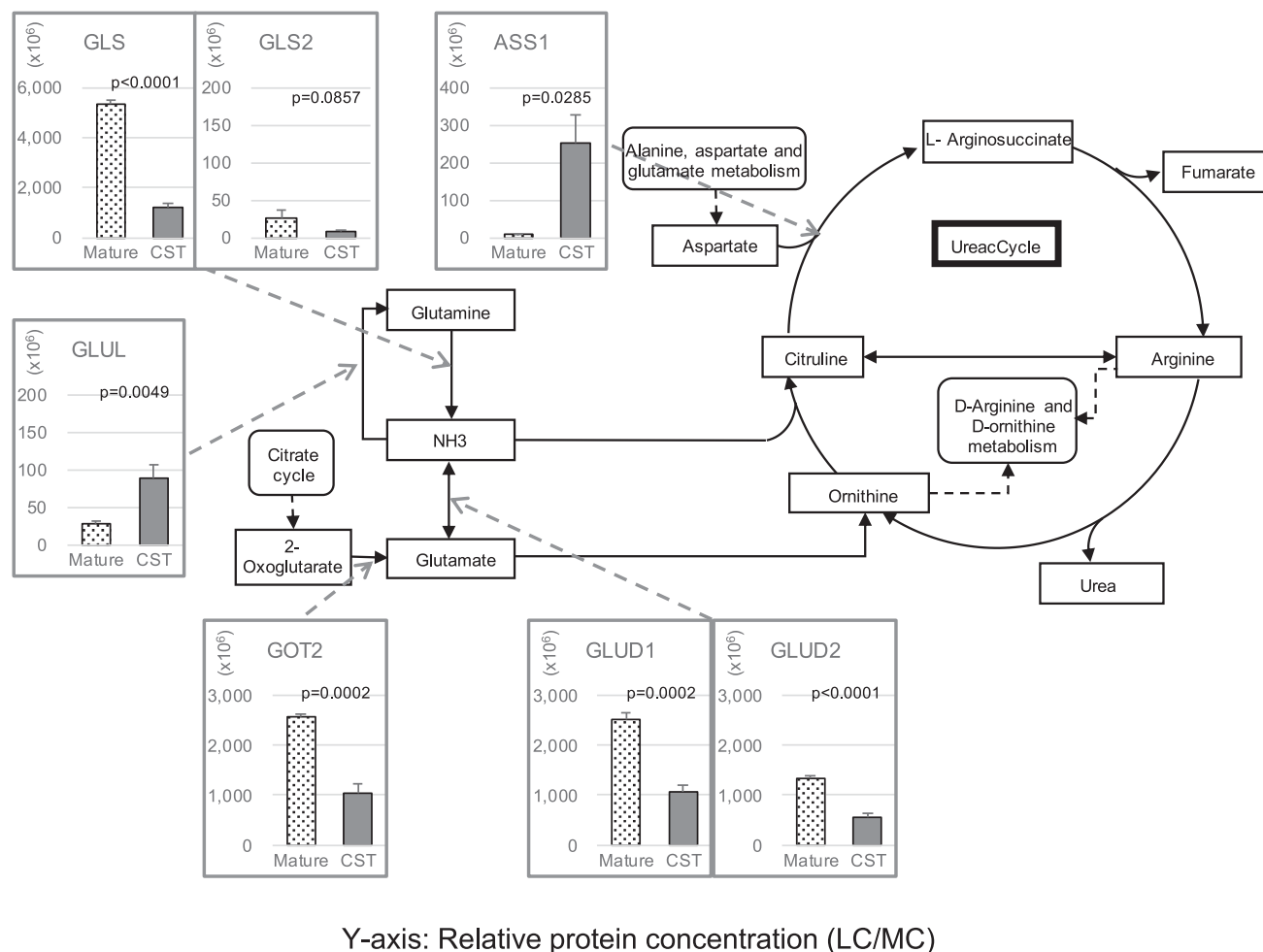
Y-axis: Relative protein concentration (LC/MC)

**FIGURE 3.** Protein expression levels of metabolites involved in arginine biosynthesis in the mature and CST cHCECs. Segregated protein expression levels of representative enzymes in arginine biosynthesis in the two types of cHCECs are illustrated on the KEGG pathway map. The average expression abundances of three lots of mature cHCECs and CST cHCECs are shown. The significance of difference between the two types of cHCECs was assessed by Student's *t*-tests after confirmation by *F* tests. *P* < 0.01 was considered statistically significant. GOT1,2, glutamic-oxaloacetic transaminase 1 and 2.

CA2 and CA3 were higher than that of CA5B. No statistically significant difference was found in CA2 and CA3 between the two types of cHCECs investigated (Fig. 5a). In addition, no expression of CA5B was detected in the CST cHCECs, compared with the moderate expression level of CA5B in the mature cHCECs, thus indicating the possible relevance of the transporter CA5B, together with SLC4A4/NBCe1, SLC4A11, and SLC9A1/NHE1, for maintaining pHi homeostasis.

## Monocarboxylate Acid Transporter (MCT)/SLC16 Family

In glycolysis, most glucose carbon is converted to pyruvate, and this pyruvate is NADH-dependently reduced to lactate by LDH.[26] The bidirectional monocarboxylate acid transporters (MCTs) perform an $H^+$-linked transport of lactate across the plasma membrane.[27] Among MCTs, MCT1 is the main lactate exporter under normal conditions, when the intracellular lactate levels are low. Between the two types of cHCECs in this study, we found that MCT1 and MCT4 protein expression levels in the cHCECs were almost at comparable

levels (Fig. 5b), although the subcellular localization of these transporters, including apical or basolateral, was not clear. MCT8 expression was detected only in the mature cHCECs (Fig. 5b). SLC5A8, a molecule recently identified as a $Na^+$-coupled transporter for short-chain monocarboxylates and known as a tumor suppressor,[28,29] was not detected in either type of cHCEC in the present proteome analysis.

## SLC12 Family and Other SLC Molecules

SLCs are the largest group of transporters in the human genome, and many SLCs reportedly play roles in cellular processes.[30] The SLC transporter proteins exhibiting either >2 or <0.5 abundance ratios—(abundance in CST cHCECs)/(abundance in the mature cHCECs)—are summarized in the Table.

Among the SLC12 family of chloride transporters, we found that A4, A5, and A6 were more highly expressed in the CST cHCECs than in the mature cHCECs, whereas A2 and A9 were inversely more highly expressed in the mature cHCECs (Fig. 6a). It is of note that A1 was detected only in the mature cHCECs. A1, also known as NKCC2, is an
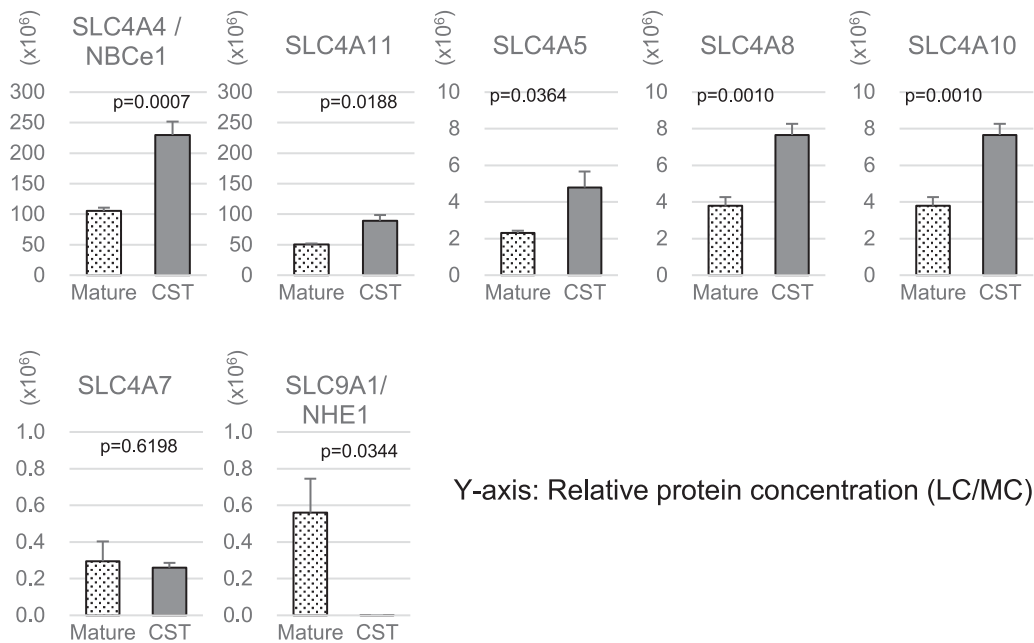
**FIGURE 4.** Protein expression of SLC4 family transporters and NHE1 in the mature and CST cHCECs. Segregated protein expression levels of representative SLC4 family transporters and NHE1 in the two types of cHCECs are illustrated. The average expression abundances of three lots of mature cHCECs and CST cHCECs are shown. The significance of difference between the two types of cHCECs was assessed by Student's *t*-tests after confirmation by *F* tests. $P < 0.01$ was considered statistically significant. The expressions of SLC4A4, A5, A10, and A11 were significantly upregulated in the CST cHCECs. SLC9A1 (NHE1) was detected only in the mature cHCECs. SLC4A1AP, solute carrier family 4 member 1 adaptor protein.

$Na^+/K^+/2Cl^-$ cotransporter, and A4, A5, and A6 function as $Na^+$-independent cation-chloride cotransporters.[31–33]

Our findings show that 17A5 and 7A14 were dominantly expressed in the mature cHCECs (Fig. 6b). SLC17A5 is an $H^+$/nitrate cotransporter, and 7A14 is a cationic amino acid transporter. SLC38A9 and 29A1 were inversely expressed dominantly in CST cHCECs (Fig. 6b). SLC38A9 is known to be a sodium-coupled neutral amino acid transporter, and 7A14 is a nucleoside transporter referred to as equilibrative nucleoside transporter 1; they both play a role in the promotion of cell proliferation.

SLC family 25 (SLC25) is comprised of a large group of proteins that transport a variety of substrates across the inner mitochondrial membrane,[34,35] and we found that SLC25A42 and A18 were selectively expressed in the mature cHCECs (Table). Interestingly, both transporters, as well as CA5, are located on the mitochondrial inner membrane.[36,37] It is well known that SLC25A42 protein is a mitochondrial transporter for cofactor coenzyme A (CoA) and ADP,[36] and SLC25A18 is a mitochondrial glutamate carrier 2, alternatively termed glutamate/H(+) symporter 2.[37]

## pHi in Distinct cHCECs

In a recent study,[15] our findings confirmed that the metabolic rewiring in the mature cHCECs provides essential cues underlying the dynamics of cell-fate modulation; however, and to the best of our knowledge, there have been no published reports with regard to a link between the metabolic rewiring of cHCECs and pHi homeostasis. The polarized expression of ion channels and SLC family transporters on two types of cHCECs may possibly indicate that the mature- and CST cHCECs can be distinguishable by their pHi. We performed a preliminary study to confirm the difference between pHi in the mature cHCECs suitable for therapy and that of the CST cHCECs, the two types of cHCECs that were provided for the analysis (Fig. 7). pHi was found to be lower in the mature cHCECs ($7.09 \pm 0.156$; n = 24) than in the CST cHCECs ($7.35 \pm 0.228$, n = 12) ($P = 0.003966$, Mann–Whitney *U* test). Phase contrast microscopy examination (Fig. 7) revealed smaller sized cells in the mature cHCECs than in the CST cHCECs, consistent with the findings of ECD being higher in the mature cHCECs (i.e., 1900 cells/mm$^2$) than in the CST cHCECs (i.e., 1231 cells/mm$^2$).

## DISCUSSION

In a previous study, we reported that, aside from that needed to meet the absolute requirements, the sole expression of $Na^+/K^+$-ATPase in cHCECs does not ensure the quality of mature differentiated CD44$^{-/+}$ cHCECs that are indispensable for cell-injection therapy for CE disorders.[1,2] In this present study, the expression of the isoforms of $Na^+/K^+$-ATPase was found to be more elevated in the mature cHCECs, leading to the speculation that pump function in the mature cHCECs may be superior to that in CST cHCECs (Fig. 1). To confirm such speculation, actual measurement of Na, K-ATPase activity or corneal endothelial pump function is required. In their excellent research on the ion (e.g., bicarbonate) channels in CE, Bonanno and associates[38,39] presented novel findings suggesting that the passive fluid influx, or "leak," is offset by an outward active "pump" located within the CE, thereby maintaining corneal hydration and transparency. The activity of basolateral $Na^+/K^+$-ATPase, $1Na^+:2HCO_3^-$ cotransport, $1Na^+:1K^+:2Cl^-$ cotransport, $Cl^-/HCO_3^-$ exchange, and $Na^+/H^+$ exchange was also confirmed.[23,25,32,40,41] Recently, Bonanno's team reported

a



Localization:

| Cytoplasm | Mitochondrial membrane | Plasma membrane |

Y-axis: Relative protein concentration (LC/MC)
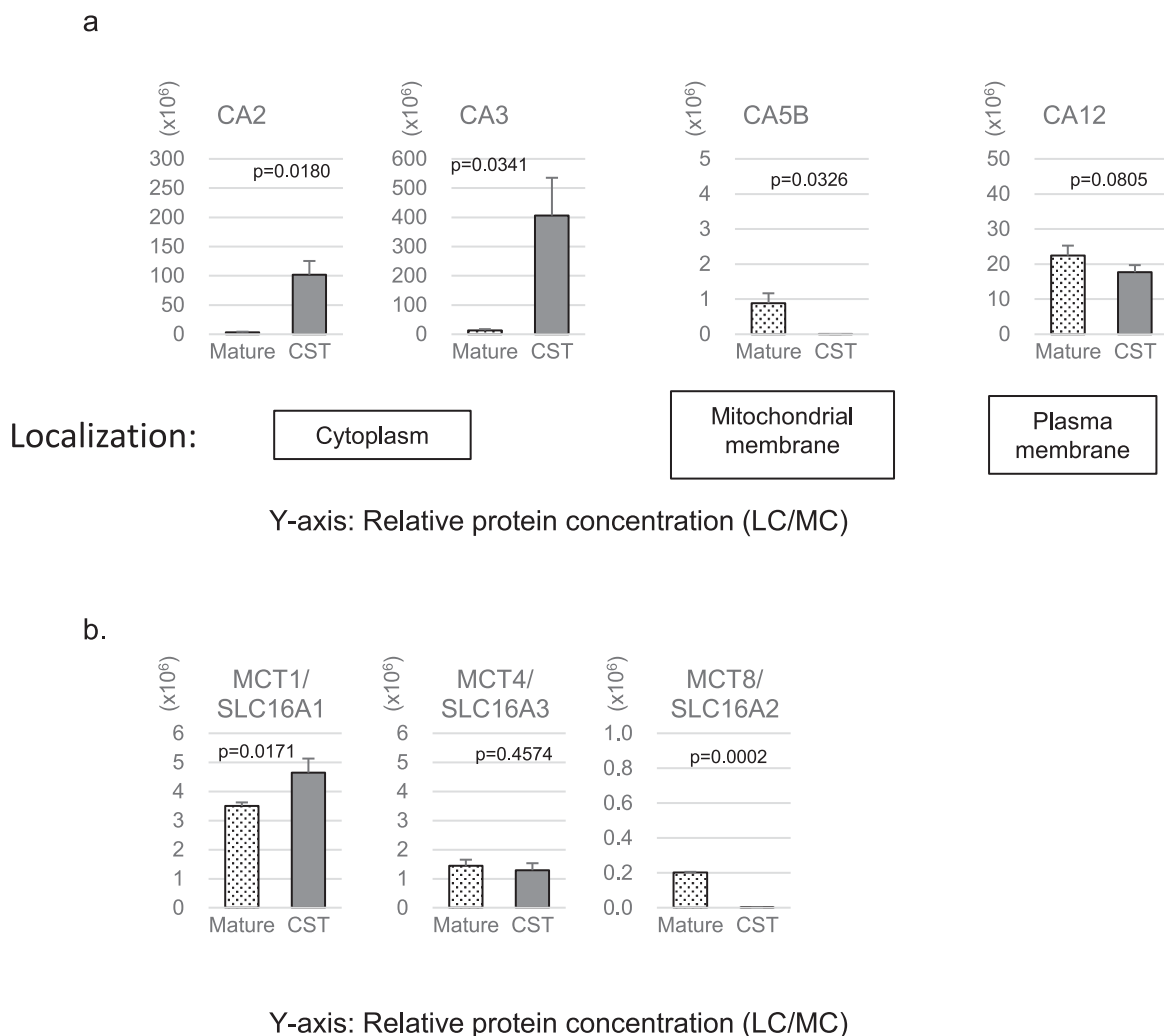
b.



Y-axis: Relative protein concentration (LC/MC)

**Figure 5.** Protein expression levels of CAs and MCTs in the mature and CST cHCECs. Segregated protein expression levels of representative CAs (**a**) and MCTs (**b**) in the two types of cHCECs are shown. The average expression abundances of three lots of mature cHCECs and CST cHCECs are shown. The significance of difference between the two types of cHCECs was assessed by Student's *t*-tests after confirmation by *F* tests. $P < 0.01$ was considered statistically significant. The selective localization of the CAs, cytosol, mitochondrial membrane, and plasma membrane is indicated. CA5B was not detected in the CST cHCECs, and MCT8 was not detected in the CST cHCECs.

that efficient Na,K-ATPase activity is necessary for maintaining the transendothelial lactate flux.[5]

$NAD^+$, which is required for the ATP-generating steps of glycolysis, is regenerated from NADH by mitochondrial NADH dehydrogenase or LDH. We found that the enzymes responsible for nicotinate and nicotinamide metabolism (i.e., NAMPT, PNP, NNMT, and NAPRT) were all upregulated in the CST cHCECs (Fig. 2). This may indicate a counter response against elevated cellular (oxidative) stress in CST cHCECs. Considering the recent identification of SLC12A8 as an NMN transporter and the requirement of sodium ion for the transport,[18] SLC12A8 may play a critical role in regulating $NAD^+$, as well as in cHCECs. However, the expression of SLC12A8 protein was not detected in our present experiment (Table), possibly due to the culture microenvironments that we adapted. The elevated expression of NAMPT (Fig. 2), the rate-limiting $NAD^+$ biosynthetic enzyme, in CST cHCECs may assist the $NAD^+$ biosynthesis itself, rather than an import from the outside. In glycolysis, most glucose carbon

is converted to pyruvate and NADH-dependent reduction of pyruvate to lactate by LDH. This reductive reaction may be what recycles the NAD+ reduced to NADH during glycolysis in cHCECs.

The metabolic programs that support cell proliferation reportedly rewire the cell-fate decisions with distinct metabolic features that may actually represent specialized adaptations to unique cellular demands.[42,43] Cell homogeneity is one of the most critical and indispensable issues for a safe, effective, and stable cell-based therapy. We previously identified one specified differentiated/mature cHCEC that shares the surface phenotypes with mature HCECs in in vivo CE tissues and found it to be an ideal cHCEC that is efficient in cell-injection therapy for CE dysfunctions[1−3] (see also Ueno M, American Academy of Ophthalmology Annual Meeting, October 12, 2019, AAO E-Poster and Abstract, PO070). It should be noted that the homeostatic cellular identity of cHCECs may require a passive metabolic adaptation to environmental culture conditions. The metabolic
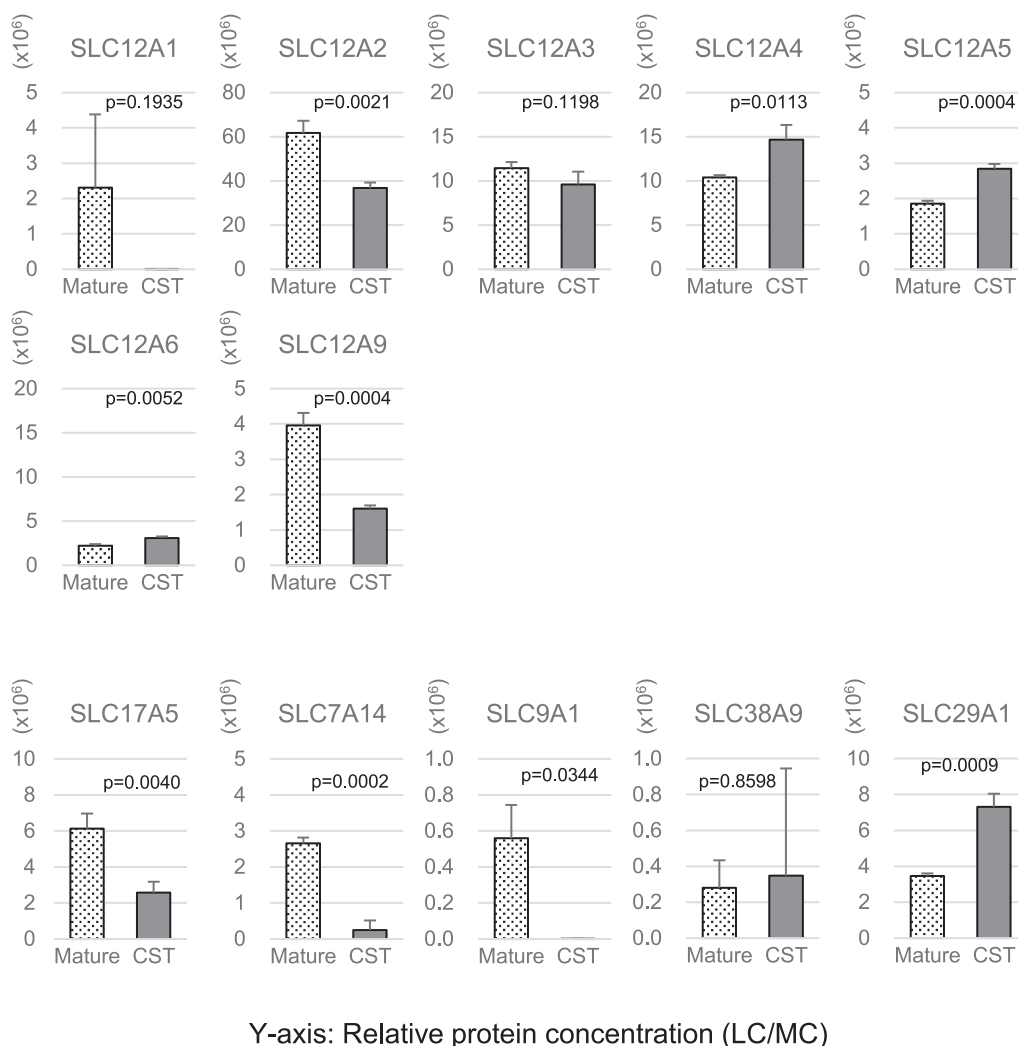
Investigative Ophthalmology & Visual Science

TABLE. Mature and CST cHCEC Abundance Ratios for SLC Transporter Family Proteins

**Average Abundance Ratio (CST/Mature) > 2**

| SLC | CD44++/+++ CST | CD44-/+ Mature | Abundance Ratio of CST/Mature |
|---|---|---|---|
| SLC38A9 | 1,038,741 | 279,670 | 3.79 |
| SLC29A1 | 7,308,576 | 3,455,069 | 2.34 |
| SLC4A4 | 229,542,708 | 105,500,458 | 2.30 |
| SLC4A8 | 7,656,416 | 3,796,133 | 2.01 |
| SLC4A10 | 7,656,416 | 3,796,133 | 2.01 |

**Average Abundance Ratio (CST/Mature) < 0.5**

| SLC | CD44++/+++ CST | CD44-/+ Mature | Abundance Ratio of CST/Mature | SLC | CD44++/+++ CST | CD44-/+ Mature | Abundance Ratio of CST/Mature |
|---|---|---|---|---|---|---|---|
| SLC25A20 | 6,639,090 | 15,657,043 | 0.50 | SLC25A13 | 57,648,687 | 183,959,205 | 0.33 |
| SLC25A31 | 84,494,219 | 166,168,896 | 0.50 | SLC25A10 | 8,528,975 | 23,584,455 | 0.32 |
| SLC25A5 | 59,082,701 | 125,582,119 | 0.47 | SLC7A14 | 244,597 | 2,651,013 | 0.23 |
| SLC25A6 | 298,085,421 | 637,430,466 | 0.46 | SLC9A1 | <1000 | 560,043 | 0.01 |
| SLC26A11 | 173,655 | 402,059 | 0.46 | SLC44A1 | <1000 | 252,736 | 0.01 |
| SLC27A1 | 239,109 | 915,164 | 0.44 | SLC2A13 | <1000 | 358,625 | 0.01 |
| SLC25A44 | 252,302 | 594,141 | 0.44 | SLC12A1 | <1000 | 3,460,743 | 0.01 |
| SLC12A9 | 1,599,000 | 3,961,037 | 0.42 | SLC25A42 | <1000 | 122,509 | 0.01 |
| SLC25A3 | 140,545,606 | 345,073,331 | 0.41 | SLC25A18 | <1000 | 78,877 | 0.01 |
| SLC38A7 | 200,046 | 538,630 | 0.38 | SLC4A1AP | <1000 | 4,246,087 | 0.01 |
| SLC3A2 | 1,940,976 | 6,627,101 | 0.37 | SLC16A2 | <1000 | 202,342 | 0.01 |
| SLC17A5 | 2,566,155 | 6,130,425 | 0.36 | | | | |

An abundance ratio of <1.000 means no detection in CST cHCECs. Thus, the abundance ratios for CST cHCECs/mature cHCECs were arbitrarily calculated as 0.01. The 52 proteins showing abundance ratios between 0.5 and 2.0 are not shown.

**Y-axis: Relative protein concentration (LC/MC)**

**Figure 6.** Protein expression levels of the SLC12 family and other SLC molecules in the mature and CST cHCECs. Segregated protein expression levels of representative CAs (**a**) and MCTs (**b**) in the two types of cHCECs are shown. The average expression abundances of three lots of mature cHCECs and CST cHCECs are shown. The significance of difference between the two types of cHCECs was assessed by Student's *t*-tests after confirmation by *F* tests. $P < 0.01$ was considered statistically significant. SLC12A1 and 9A1 were not detected in the CST cHCECs.

convergence between proliferation and cell-fate regulation may be relevant in immature cHCECs, as is the case in stem cells.[42]

Of interest, distinct metabolic features can be characterized in terms of the functional expression of ion channels and diverse transporters among cHCECs with high metabolic activity. Lactate/$H^+$ cotransport via MCTs is facilitated by $HCO_3^-$, CA activity, $Na^+/H^+$ exchange, and $1Na^+{:}2HCO_3^-$ cotransport.[44] This indicates that the efficient reduction of intracellular lactate is essential in lowering corneal hydration, thus suggesting that cellular buffering by $HCO_3^-$, $HCO_3^-$ transporters, and CA activity might be a significant component of the CE pump that reduces the risk of corneal edema by maintaining a low level of stromal lactate.[40] We found that CD44[++/+++] CST cHCECs display segregated profiles of extracellularly secreted metabolites (i.e., an increased amount of lactic acid and TCA-cycle intermediates), whereas secreted serine and branched-chain amino acids were decreased in the mature cHCECs.[15]

Also of interest, we found that most enzymes with mitochondrial localization were upregulated in the mature cHCECs, whereas most enzymes with cytosolic localization were upregulated in the CD44[++/+++] CST cHCECs.[15] To maintain the physiological pHi homeostasis, cells reportedly require the efflux of lactate and $H^+$ to prevent intracellular acidification.[45,46] Among the cHCECs in this study, MCT1 and MCT4 protein expression was unexpectedly almost at comparable levels in the mature cHCECs and the CST cHCECs (Fig. 5b). Hence, it may be critical to further clarify the subcellular localization, including either apical or basolateral, in future studies. A recent report described the relevance of concerted actions for the differentiation in mature adipocytes through upregulated MCT1- and MCT4-mediated lactate flux and NBCe1 (SLC4A4)-mediated $HCO_3^-$/pH homeostasis,[47] which may imply the relevance of similar concerted actions in the differentiation of cHCECs. Moreover, polarized expression of MCT has been reported, with studies describing MCT1, MCT2, and MCT4 being expressed in rabbit CE on both the apical and basolateral cell

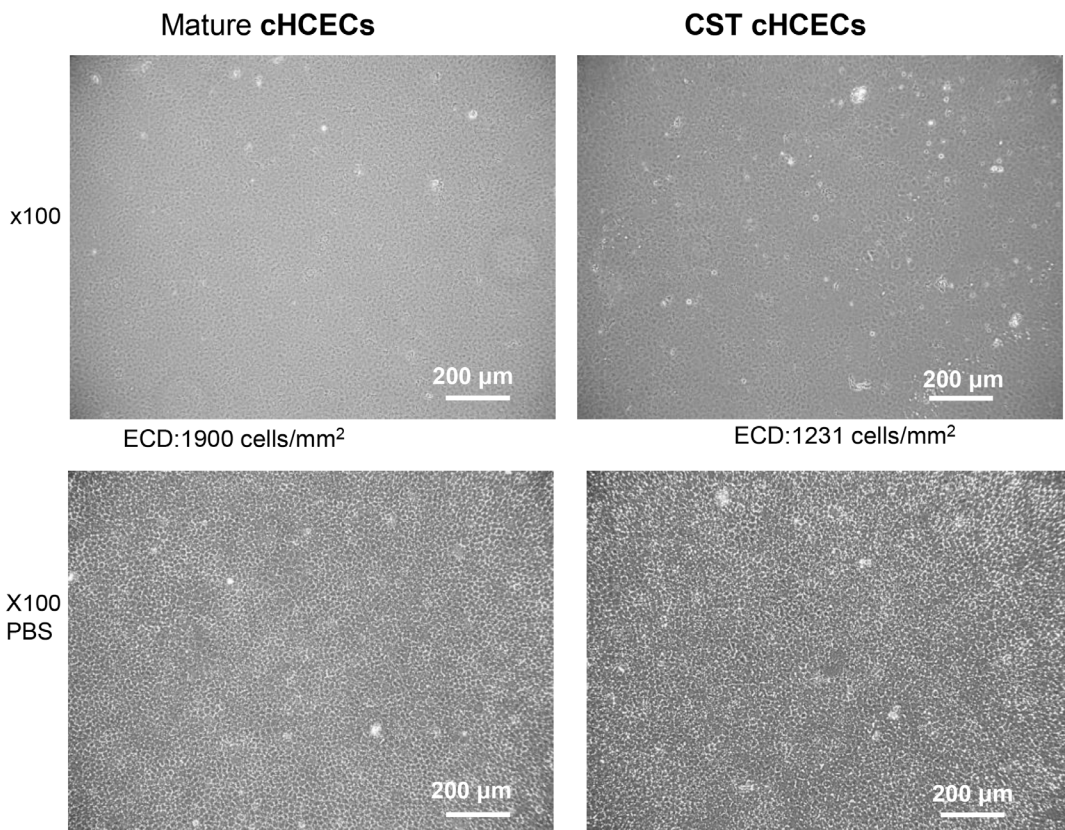## a. FACS
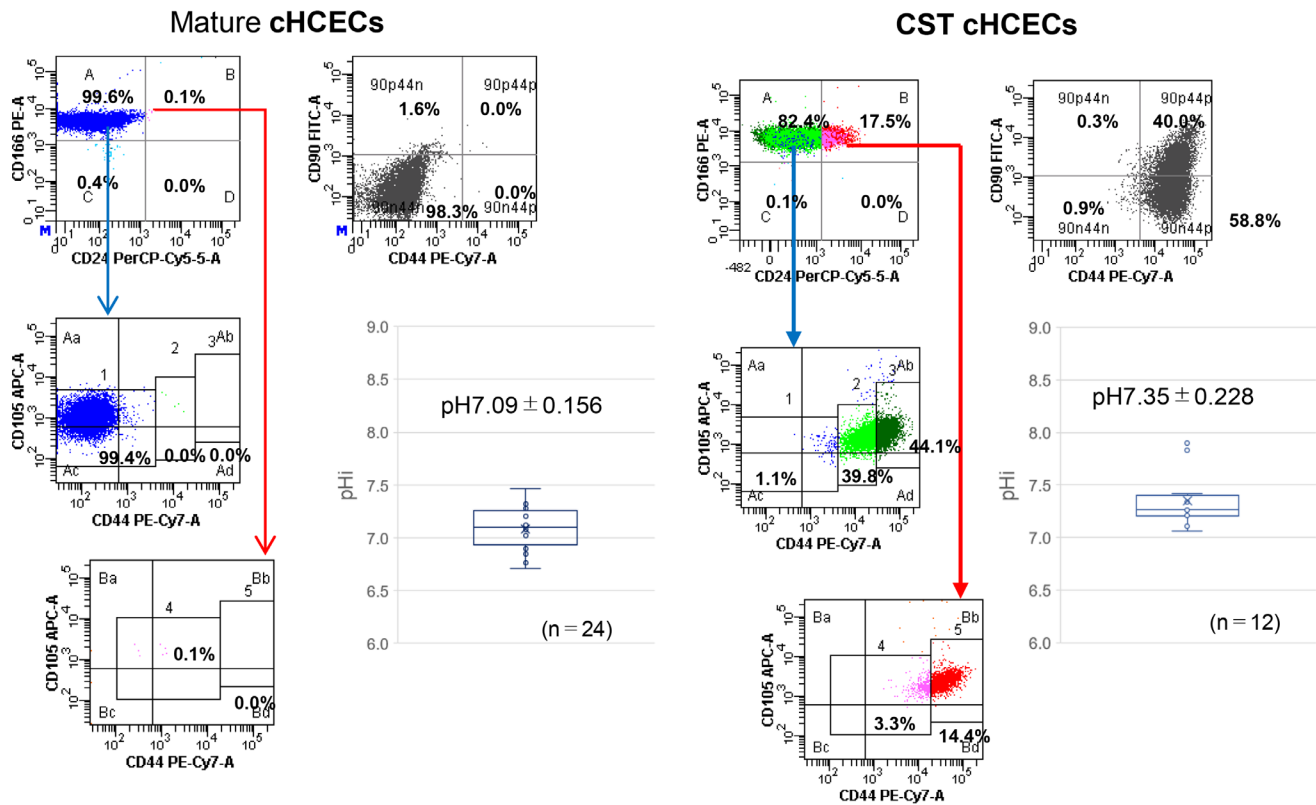


## b. Phase contras microscopy



**FIGURE 7.** pHi in the mature and CST cHCECs. A lower pHi was found in the mature cHCECs ($7.09 \pm 0.156$) compared to the CST cHCECs ($7.35 \pm 0.228$) ($P = 0.003966$, Mann–Whitney $U$ test). Phase contrast microscopy imaging revealed smaller sized cells in the mature cHCECs

compared to the CST cHCECs. The corneal ECD was 1900 cells/mm$^2$ in the mature cHCECs and 1231 cells/mm$^2$ in the CST cHCECs. (**a**) Fluorescence-activated cell-sorting (FACS) analysis. (**b**) Phase contrast microscopy images of the cultures on day 40 at the end of the passage 4 (*upper*) and after PBS treatments to clearly define the cell boundaries.

surface.[48] Also, the cellular buffering contributed by $HCO_3^-$, NBCe1, and CA activity facilitates lactate/$H^+$ efflux, thus controlling corneal hydration in in vivo basolateral surfaces and function to transport lactate/$H^+$.[49] These findings may imply the relevance of similar concerted actions in the differentiation of cHCECs. Although the function of MCT8 as a transporter of thyroid hormones is well known in other cells, the exact function of MCT8 in the physiological pHi homeostasis of cHCECs has yet to be elucidated.[50]

NHEs have multiple functions in pathological and physiological processes, including regulation of NaCl transport, intracellular acid–base balance, pH homeostasis, and, consequently, cell volume.[51–53] The $Na^+/H^+$ exchange activity of NHE1 is crucial for pHi regulation, and, quite strikingly, we found that NHE1 was expressed only in the mature cHCECs. Activation of NHE1 by osmotic stress or intracellular acidification and inhibition of NHE1 by ATP depletion occur without detectable changes in the phosphorylation of the exchanger.[54] The stress of accelerated lactate production in glycolysis in CD44$^{++/+++}$ CST cHCECs would not be compensated in the context of MCT, and the pHi homeostasis might be fragile. For example, it was reported that p38 mitogen-activated protein kinase-dependent phosphorylation of NHE1 could be activated by platelet-derived growth factorin culture medium,[54–56] thus implying the metabolic fragility of cHCECs and substantial interference with the control of cell quality.

A TCA cycle supported by glutamine was reportedly found to involve the supply of acetyl CoA to the TCA cycle.[44] Glutaminolysis, which is needed to maintain CE function, is severely disrupted in CE cells deficient in $NH_3/H^+$ cotransporter SLC4A11.[14] In a study by Guha et al.,[57] the authors suggested a possible role of SLC4A11 in regulating oxidative stress. In this present study, we found that many of the SLC4 family members were upregulated in the CST cHCECs (Fig. 4). In a recent study, it was reported that the export of $NH3^+$ through SLC4A11 confers the proliferative features to the corresponding cells.[58] It is of note that the SLC4A11 gene is responsible for late-onset Fuchs corneal dystrophy, congenital hereditary endothelial dystrophy, and posterior polymorphous corneal dystrophy and has been applied in the treatment of corneal endothelial dystrophy.[19,59]

In addition to the polarized presence of NHE1 in the mature cHCECs, our findings, interestingly, confirmed the polarized presence of mitochondria localized isoforms of transporters CA5, SLC25A42, and SLC25A18 only in the mature cHCECs. All of these isoforms are relevant to providing substrates for mitochondrial respiration (Figs. 4, 5, 6). Reportedly, the most important function of CAs is related to the respiration and transport of $CO_2$/bicarbonate in various tissues,[60] and the primary function of SLC25A42 is probably to catalyze the entry of CoA into the mitochondria in exchange for adenine nucleotides.[37] SLC25A18 reportedly functions as a mitochondrial glutamate carrier 2 and may play a role in glutamine-mediated anaplerosis.[37] Furthermore, in this study, the observed polarized presence of transporters that provide the mitochondrial substrates was also confirmed in HCE tissues with regard to ECD in CE tissues. The expres-

sion of CA5 and SLC25A42 was higher in HCE tissues with an ECD of >3000. Conversely, the expression of SLC25A18, a mitochondrial glutamate carrier 2, was higher in HCE tissues with an ECD of <2000 (Supplementary Fig. S3).

Divergent energetic requirements among heterogeneous cHCECs may implicate either a segregated metabolic profile or distinct mitochondrial function among the mature, immature, and CST cHCECs. Alterations in the metabolic features in the context of polarized expression of ion channels and SLC family transporters are consistent with our previous observation that mature differentiated cHCECs become more oxidative and elicit a reduced amount of lactate secretion extracellularly, thus providing additional, relevant qualification markers to identify heterogeneous cHCECs suitable for cell-injection therapy. In the near future, it will be necessary to conduct an intensive study to validate these findings and confirm the functional activity of the components described in this study.

In conclusion, the findings presented in this study clearly indicate the necessity for much more extensive and detailed studies regarding this new aspect of ion channels and transporter-like proteins expressed in cHCECs. Further intensive research is needed to provide new molecular targets beyond cell-based therapy for CE disorders and to provide a better understanding of the underlying molecular mechanism in the differentiation of HCECs.

Disclosure: **J. Hamuro**, None; **H. Deguchi**, None; **T. Fujita**, None; **K. Ueda**, None; **Y. Tokuda**, None; **N. Hiramoto**, None; **K. Numa**, None; **M. Nakano**, None; **J. Bush**, None; **M. Ueno**, None; **C. Sotozono**, None; **S. Kinoshita**, None

## *References*

1. Kinoshita S, Koizumi N, Ueno M, et al. Injection of cultured cells with a ROCK inhibitor for bullous keratopathy. *N Engl J Med*. 2018;378:995–1003.

2. Hamuro J, Toda M, Asada K, et al. Cell homogeneity indispensable for regenerative medicine by cultured human corneal endothelial cells. *Invest Ophthalmol Vis Sci*. 2016;57:4749–4761.

3. Toda M, Ueno M, Hiraga A, et al. Production of homogeneous cultured human corneal endothelial cells indispensable for innovative cell therapy. *Invest Ophthalmol Vis Sci*. 2017;58:2011–2020.

4. Hamuro J, Ueno M, Asada K, et al. Metabolic plasticity in cell state homeostasis and differentiation of cultured

human corneal endothelial cells. *Invest Ophthalmol Vis Sci.* 2016;57:4452–4463.

5. Li S, Kim E, Ogando DG, Bonanno JA. Corneal endothelial pump coupling to lactic acid efflux in the rabbit and mouse. *Invest Ophthalmol Vis Sci.* 2020;61:7.

6. Laing RA, Chiba K, Tsubota K, Oak SS. Metabolic and morphologic changes in the corneal endothelium. The effects of potassium cyanide, iodoacetamide, and ouabain. *Invest Ophthalmol Vis Sci.* 1992;33:3315–3324.

7. Greiner MA, Burckart KA, Wagoner MD, et al. Assessment of energy-producing metabolic activity in the endothelium of donor corneas. *Invest Ophthalmol Vis Sci.* 2015;56:2803–2810.

8. Herrera AS, Del CA Esparza M, Ashraf G, Zamyatnin AA, Aliev G. Beyond mitochondria, what would be the energy source of the cell? *Cent Nerv Syst Agents in Med Chem.* 2015;15:32–41.

9. Tatsuta T, Langer T. Quality control of mitochondria: protection against neurodegeneration and ageing. *EMBO J.* 2008;27:306–314.

10. Youle RJ, van der Bliek AM. Mitochondrial fission, fusion, and stress. *Science.* 2012;337:1062–1065.

11. Wilson DF. Oxidative phosphorylation: regulation and role in cellular and tissue metabolism. *J Physiol.* 2017; 595:7023–7038.

12. Wallace DC. Mitochondria and cancer. *Nat Rev Cancer.* 2012;12:685–698.

13. Li S, Kim E, Bonanno JA. Fluid transport by the cornea endothelium is dependent on buffering lactic acid efflux. *Am J Physiol Cell Physiol.* 2016;311:C116–C126.

14. Zhang W, Li H, Ogando DG, et al. Glutaminolysis is essential for energy production and ion transport in human corneal endothelium. *EBioMedicine.* 2017;16:292–301.

15. Hamuro J, Numa K, Fujita T, et al. Metabolites interrogation in cell fate decision of cultured human corneal endothelial cells. *Invest Ophthalmol Vis Sci.* 2020;61:10.

16. Wang YH, Israelsen WJ, Lee D, et al. Cell-state-specific metabolic dependency in hematopoiesis and leukemogenesis. *Cell.* 2014;158:1309–1323.

17. Li L, Mao Y, Zhao L, et al. P53 regulation of ammonia metabolism through urea cycle controls polyamine biosynthesis. *Nature.* 2019;567:253–256.

18. Grozio A, Mills KF, Yoshino J, et al. Slc12a8 is a nicotinamide mononucleotide transporter. *Nat Metab.* 2019;1:47–57.

19. Eghrari AO, Riazuddin SA, Gottsch JD. Fuchs corneal dystrophy. *Prog Mol Biol Transl Sci.* 2015;134:79–97.

20. Yoshino J, Mills KF, Yoon MJ, Imai S. Nicotinamide mononucleotide, a key NAD+ intermediate, treats the pathophysiology of diet- and age induced diabetes in mice. *Cell Metab.* 2011;14:528–536.

21. Garten A, Schuster S, Penke M, Gorski T, de Giorgis T, Kiess W. Physiological and pathophysiological roles of NAMPT and NAD metabolism. *Nat Rev Endocrinol.* 2015;11:535–546.

22. Imai S. Nicotinamide phosphoribosyltransferase (Nampt): a link between NAD biology, metabolism, and diseases. *Curr Pharm Des.* 2009;15;20–28.

23. Malhotra D, Loganathan SK, Chiu AM, Lukowski CM, Casey JR. Human corneal expression of SLC4A11, a gene mutated in endothelial corneal dystrophies. *Sci Rep.* 2019;9: 9681.

24. Counillon L, Bouret Y, Marchiq I, Pouysségur J. Na (+)/H (+) antiporter (NHE1) and lactate/H (+) symporters (MCTs) in pH homeostasis and cancer metabolism. *Biochim Biophys Acta.* 2016;1863:2465–2480.

25. Bonanno JA. Molecular mechanisms underlying the corneal endothelial pump. *Exp Eye Res.* 2012;95:2–7.

26. DeBerardinis RJ, Lum JJ, Hatzivassiliou G, Thompson CB. The biology of cancer: metabolic reprogramming fuels cell growth and proliferation. *Cell Metab.* 2008;7:11–20.

27. Halestrap AP. The SLC16 gene family - structure, role and regulation in health and disease. *Mol Aspects Med.* 2013;34:337–349.

28. Bhutia YD, Babu E, Ramachandran S, Yang S, Thangaraju M, Ganapathy V. SLC transporters as a novel class of tumour suppressors: identity, function and molecular mechanisms. *Biochem J.* 2016;473:1113–1124.

29. Gupta N, Martin PM, Prasad PD, Ganapathy V. SLC5A8 (SMCT1)-mediated transport of butyrate forms the basis for the tumor suppressive function of the transporter. *Life Sci.* 2006;78:2419–2425.

30. Hägglund MG, Sreedharan S, Nilsson VC, et al. Identification of SLC38A7 (SNAT7) protein as a glutamine transporter expressed in neurons. *J Biol Chem.* 2011;286:20500–20511.

31. Hebert SC, Mount DB, Gamba G. Molecular physiology of cation-coupled Cl-cotransport: the SLC12 family. *Pflügers Arch.* 2004;447:580–593.

32. Markadieu N, Delpire E. Physiology and pathophysiology of SLC12A1/2 transporters. *Pflügers Arch.* 2014;466:91–105.

33. Gagnon KB, Di Fulvio M. A molecular analysis of the Na(+)-independent cation chloride cotransporters. *Cell Physiol Biochem.* 2013;32:14–31.

34. Palmieri F. The mitochondrial transporter family SLC25: identification, properties and physiopathology. *Mol Aspects Med.* 2013;34:465–484.

35. Wang YJ, Khan FI, Xu Q, Wei DQ. Recent studies of mitochondrial SLC25: integration of experimental and computational approaches. *Curr Protein Pept Sci.* 2018;19:507–522.

36. Fiermonte G, Paradies E, Todisco S, Marobbio CM, Palmieri F. A novel member of solute carrier family 25 (SLC25A42) is a transporter of coenzyme A and adenosine 3′,5′-diphosphate in human mitochondria. *J Biol Chem.* 2009;284:18152–18159.

37. Porcelli V, Longo A, Palmieri L, Closs EI, Palmieri F. Asymmetric dimethylarginine is transported by the mitochondrial carrier SLC25A2. *Amino Acids.* 2016;48:427–436.

38. Nguyen TT, Bonanno JA. Lactate-H$^+$ transport is a significant component of the in vivo corneal endothelial pump. *Invest Ophthalmol Vis Sci.* 2012;53:2020–2029.

39. Bonanno JA. Identity and regulation of ion transport mechanisms in the corneal endothelium. *Prog Retin Eye Res.* 2003;22:69–94.

40. Bonanno JA, Giasson C. Intracellular pH regulation in fresh and cultured bovine corneal endothelium. I. Na+/H+ exchange in the absence and presence of HCO$_3^-$. *Invest Ophthalmol Vis Sci.* 1992;33:3058–3067.

41. Adijanto J, Philp NJ. The SLC16A family of monocarboxylate transporters (MCTs)–physiology and function in cellular metabolism, pH homeostasis, and fluid transport. *Curr Top Membr.* 2012;70:275–311.

42 Intlekofer AM, Finley LWS. Metabolic signatures of cancer cells and stem cells. *Nat Metab.* 2019;1:177–188.

43. Le A, Lane A, Hamaker M, et al. Glucose-independent glutamine metabolism via TCA cycling for proliferation and survival in B cells. *Cell Metab.* 2012;15:110–121.

44. Nguyen TT, Bonanno JA. Bicarbonate, NBCe1, NHE, and carbonic anhydrase activity enhance lactate-H+ transport in bovine corneal endothelium. *Invest Ophthalmol Vis Sci.* 2011;52:8086–8093.

45 Ryan DG, Murphy MP, Frezza C, et al. Coupling Krebs cycle metabolites to signaling in immunity and cancer. *Nat Metab.* 2019;1:16–33.

46. Benjamin D, Robay D, Hindupur SK, et al. Dual inhibition of the lactate transporters MCT1 and MCT4 is synthetic lethal

with metformin due to NAD+ depletion in cancer cells. *Cell Rep*. 2018;25:3047–3058.e4.

47. Petersen C, Nielsen MD, Andersen ES, et al. MCT1 and MCT4 expression and lactate flux activity increase during white and brown adipogenesis and impact adipocyte metabolism. *Sci Rep*. 2017;7:13101.

48. Li S, Nguyen TT, Bonanno JA. CD147 required for corneal endothelial lactate transport. *Invest Ophthalmol Vis Sci*. 2014;55:4673–4681.

49. Nguyen TT, Bonanno JA. Lactate-H$^+$ transport is a significant component of the in vivo corneal endothelial pump. *Invest Ophthalmol Vis Sci*. 2012;53:2020–2029.

50. Liu YY, Brent GA. Thyroid hormone and the brain: mechanisms of action in development and role in protection and promotion of recovery after brain injury. *Pharmacol Ther*. 2018;86:176–185.

51. Lee SH, Kim T, Park ES, et al. NHE10, an osteoclast-specific member of the Na$^+$/H$^+$ exchanger family, regulates osteoclast differentiation and survival [corrected]. *Biochem Biophys Res Commun*. 2008;369:320–326.

52. Zachos NC, Tse M, Donowitz M. Molecular physiology of intestinal Na$^+$/H$^+$ exchange. *Annu Rev Physiol*. 2005;67:411–443.

53. Wang A, Li J, Zhao Y, Johansson ME, Xu H, Ghishan FK. Loss of NHE8 expression impairs intestinal mucosal integrity. *Am J Physiol Gastrointest Liver Physiol*. 2015;309:G855–G864.

54. Yan W, Nehrke K, Choi J, Barber DL. The Nck-interacting kinase (NIK) phosphorylates the Na$^+$-H$^+$ exchanger NHE1 and regulates NHE1 activation by platelet-derived growth factor. *J Biol Chem*. 2011;276:31349–31356.

55. Wang H, Silva NL, Lucchesi PA, et al. Phosphorylation and regulation of the Na$^+$/H$^+$ exchanger through mitogen activated protein kinase. *Biochemistry*. 1997;36:9151–9158.

56. Khaled AR, Moor AN, Li A, et al. Trophic factor withdrawal: p38 mitogen-activated protein kinase activities NHE1, which induces intracellular alkalinization. *Mol Cell Biol*. 2001;21:7545–7557.

57. Guha S, Chaurasia S, Ramachandran C, Roy S. SLC4A11 depletion impairs NRF2 mediated antioxidant signaling and increases reactive oxygen species in human corneal endothelial cells during oxidative stress. *Sci Rep*. 2017;7:4074.

58. Li L, Mao Y, Zhao L, et al. P53 regulation of ammonia metabolism through urea cycle controls polyamine biosynthesis. *Nature*. 2019;567:253–256.

59. Riazuddin SA, Vithana EN, Seet LF, et al. Missense mutations in the sodium borate cotransporter SLC4A11 cause late-onset Fuchs corneal dystrophy. *Hum Mutat*. 2010;31:1261–1268.

60. Imtaiyaz Hassan M, Shajee B, Waheed A, Ahmad F, Sly WS. Structure, function and applications of carbonic anhydrase isozymes. *Bioorg Med Chem*. 2013;21:1570–1582.